Proceeding of the IEEE
International Conference on Information and Automation
Hailar, China, July 2014

Design and Preliminary Experimentation of a Continuum Exoskeleton for Self-Provided Bilateral Rehabilitation

Kai Xu*, *Member, IEEE*, You Wang, and Zhixiong Yang, *Student Member, IEEE*

***Abstract*—Existing exoskeletons for rehabilitation usually consist of a rigid kinematic chain of various forms. They are often bulky in size and need structural adjustments from time to time to fit to a specific patient. This paper presents a continuum exoskeleton design for bilateral rehabilitation. Its intrinsic flexibility adapts to different patient anatomies passively to provide AAA (Anatomy Adaptive Assistances) to a group of patients without requiring any hardware adjustments. It has a unique symmetric structure which transmits the motions of the unaffected healthy side to drive the affected hemiparetic side, using the design's backdrivability. The design compactness also allows the exoskeleton to be brought home for self-provided rehabilitation exercises. The design concept, kinematics, system descriptions and preliminary experimentation are reported. With this new exoskeleton constructed, clinical effectiveness of this equipment could be evaluated and new rehabilitation strategies could be developed.**

I. Introduction

RESEARCH on exoskeleton has been active in the past decades. Many exoskeletons were developed [1]. Besides the ones for physical capability enhancement [2-5], exoskeletons are also used in rehabilitation for neuromuscular defects after injury or stroke. Examples include the ones for lower limbs [6-9], and the ones for upper limbs [10-17]. Unlike the point-reaching type of robotic rehabilitation devices (such as the ones in [18-20]), exoskeletons for rehabilitation guide the entire limb of a patient for specific training poses and provide active assistance or impedance to each individual joint. The proper use of an exoskeleton's capability could lead to better training outcomes.

Massed practice (repeated movement training) has been shown effective in rehabilitation therapy [21]. And the training strategies include explicit learning (patients fully aware of movement trajectories), implicit learning (patients' task-based movements are not directed on a conscious level) and bilateral training (symmetric movements of the paretic and healthy arms). Bilateral training generates better rehabilitation outcomes than repetitive motions (explicit and implicit) [21], because bilateral movements may stimulate functional improvements via reinforcing corticospinal links between the undamaged cortical hemisphere and the affected limb [20]. Furthermore, the undamaged hemisphere might alter the affected hemisphere through the intercallosal fibers during one's bilateral movements [22]. Findings from [23] using fMRI (functional Magnetic Resonance Imaging) also confirmed the effectiveness of bilateral training.

This paper presents the initial efforts of designing and building an upper-extremity exoskeleton for self-provided portable bilateral rehabilitation, motivated by the proven efficacy of bilateral training. The design is also intended for portability due to the recent positive results from the home-based therapies using a portable device [24]. The proof-of-concept prototype of a continuum shoulder exoskeleton is shown in Fig. 1. Design concepts, kinematics, system descriptions, and preliminary experimentation of this continuum shoulder exoskeleton are presented.

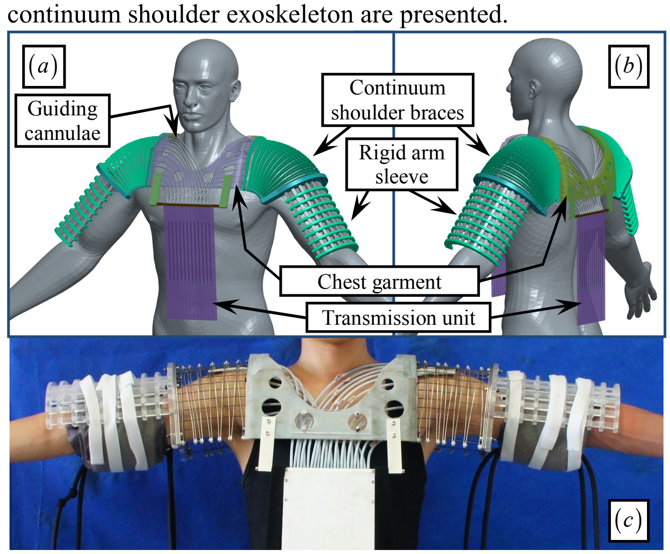

Fig. 1. The compliant continuum shoulder exoskeleton for self-provided bilateral rehabilitation: (a) the front view, (b) the back view, and (c) the prototype worn on a human subject

Unique features of this design, which could be identified as this paper's contributions, include the following two aspects.

- The continuum shoulder brace conforms to different anatomies passively, providing AAA (Anatomy Adaptive Assistances) to a group of patients without requiring any hardware adjustments. This feature is particularly useful in a clinical setting when an exoskeleton is shared by multiple patients. On the contrary, it could be challenging to maintain the kinematic compatibility between a patient with an exoskeleton made from rigid links [25, 26]. Previous attempts of using non-rigid components in exoskeleton designs include an upper body exoskeleton using home-made pneumatic artificial muscles [27], a

Manuscript received June 30*th*, 2014. This work was supported in part by the National Program on Key Basic Research Projects (Grant No. 2011CB013300), in part by the Shanghai Rising-Star Program (Grant No. 14QA1402100), and in part by the State Key Laboratory of Mechanical Systems and Vibration (Grant No. MSVZD201406).

The authors are with the RII Lab (Lab of Robotics Innovation and Intervention), UM-SJTU Joint Institute, Shanghai Jiao Tong University, Shanghai, 200240, China (asterisk indicates the corresponding author, phone: 86-21-34207220; fax: 86-21-34206525; emails: k.xu@sjtu.edu.cn, youwang@sjtu.edu.cn, and yangzhixiong@sjtu.edu.cn)

978-1-4799-4100-1/14/$31.00 ©2014 IEEE

cable-driven upper-limb exoskeleton [16, 17], and a motorized continuum shoulder exoskeleton [28, 29].
- The symmetric continuum shoulder braces are connected through the transmission units so that the motions of the unaffected healthy side are transmitted to directly drive the affected hemiparetic side. This design presents a greatly simplified scheme to realize bilateral motions. Existing systems, such as the MIME (Mirror Image Movement Enabler) [19] and the Bi-Manu-Track system [30], often use a tracking device to monitor the poses of the unaffected arm and use a robotic manipulator to drive the affected arm to produce bilateral movements.

The paper is organized as follows. Section II presents the design concept and the system overview. Section III presents nomenclature and kinematics so that the system descriptions presented in Section IV can be better elaborated. Section V presents preliminary experimentation of this continuum shoulder exoskeleton, demonstrating the realization of self-provided bilateral motions on a human subject and a mockup patient with different shoulder widths. Section VI presents conclusions and future work.

II. Design Concept and System Overview

The symmetric continuum shoulder exoskeleton shown in Fig. 1 consists of two rigid arm sleeves, two flexible continuum shoulder braces, a chest garment, sets of guiding cannulae, and two transmission units.

Structure of the continuum shoulder brace is shown in Fig. 4 with a generic structure depicted in Fig. 2. It consists of an end ring, several secondary backbones, a few spacer rings and a base ring. All the backbones are made from thin NiTi (Nickel-Titanium alloy) rods. The secondary backbones are only attached to the end ring and can slide in holes of the spacer rings and the base ring. Referring to Fig. 2, a virtual primary backbone located in the center characterizes the length and the shape of the continuum brace. The actual shape of the continuum brace depends on a minimum of the potential energy distributed along the backbones with constraints from the wearer's anatomy.

The flexible continuum shoulder brace has three DoFs (Degrees of Freedom), including a 2-DoF bending and 1-DoF extension/contraction. Push-pull actuation of these secondary backbones in a synchronized manner would bend and/or extend/shorten the continuum shoulder brace.

Bending of the continuum brace could orient a wearer's arm, which was demonstrated previously by a motorized continuum shoulder exoskeleton for delivering unilateral assistances [28, 29]. This paper builds on the existing results and uses the back-drivability of the continuum brace to realize bilateral motions. While worn on a hemiparetic patient, the unaffected arm (e.g. the right arm) could actively bend the right brace and the right-brace backbones will be pushed and pulled by the bending of the right brace. The right-brace backbones are routed through the guiding cannulae and connected to the left-brace backbones in the transmission units. Push-pull motions of the right-brace backbones are transformed to those of the left-brace backbones so as to bend the left brace and orient the left arm (e.g. the hemiparetic arm). Extension (or contraction) of the brace is also of critical importance. The reason will be elaborated in Section III.B based on the derived kinematics.

Besides the simple realization of bilateral movements, the braces adapt to different wearer anatomies passively due to the intrinsic compliance and can always assure the kinematic compatibility between the braces and a group of patients. This was confirmed by the previous experimental study in [29].

Advantages of this continuum shoulder exoskeleton design include: i) comfort and safety introduced by the inherent compliance of the continuum braces, ii) passive adaptation to different anatomies, iii) self-provided bilateral motions for rehabilitation, and iv) design compactness and portability for possible home-based therapies.

III. Nomenclature and Kinematics

The nomenclature and the kinematics assume that the continuum brace bends in a planar manner within the bending plane, as shown in Fig. 2. Shapes of the secondary backbones are assumed by a sweeping motion of the structure's cross section along the virtual primary backbone. The cross section is assumed rigid and perpendicular to the primary backbone.

A. Nomenclature

Nomenclatures are defined in Table I, while coordinate systems of the continuum brace are defined as follows:

- *Base Ring Coordinate System* (BRS) is designated as $\{b\} \equiv \{\hat{\mathbf{x}}_b, \hat{\mathbf{y}}_b, \hat{\mathbf{z}}_b\}$. It is attached to the base ring of the continuum brace, whose XY plane coincides with the base ring and its origin is at the center of the base ring. $\hat{\mathbf{x}}_b$ points from the center of the base disk to the first secondary backbone while $\hat{\mathbf{z}}_b$ is perpendicular to the base ring. Secondary backbones are numbered according to the definition of δ_i.
- *Bending Plane Coordinate System 1* (BPS1) is designated as $\{1\} \equiv \{\hat{\mathbf{x}}_1, \hat{\mathbf{y}}_1, \hat{\mathbf{z}}_1\}$ which shares its origin with $\{b\}$ and has the continuum brace bending in its XZ plane.
- *Bending Plane Coordinate System 2* (BPS2) is designated as $\{2\} \equiv \{\hat{\mathbf{x}}_2, \hat{\mathbf{y}}_2, \hat{\mathbf{z}}_2\}$ obtained from $\{1\}$ by a rotation about $\hat{\mathbf{y}}_1$ such that $\hat{\mathbf{z}}_1$ becomes backbone tangent at the end ring. Origin of $\{2\}$ is at center of the end ring.
- *End Ring Coordinate System* (ERS) $\{e\} \equiv \{\hat{\mathbf{x}}_e, \hat{\mathbf{y}}_e, \hat{\mathbf{z}}_e\}$ is fixed to the end ring. $\hat{\mathbf{x}}_e$ points from center of the end ring to the 1*st* secondary backbone and $\hat{\mathbf{z}}_e$ is normal to the end ring. $\{e\}$ is obtained from $\{2\}$ by a rotation about $\hat{\mathbf{z}}_2$.

TABLE I
Nomenclature Used in This Paper

m	Number of the secondary backbones
i	Index of the secondary backbones, $i = 1, 2, \cdots, m$
r_i	Distance from the virtual primary backbone to the *ith* secondary backbone. r_i can be different for different i.

β_i	β_i characterizes the division angle from the *ith* secondary backbone to the 1*st* secondary backbone. $\beta_1 \equiv 0$ and β_i remain constant once the brace is built.
L, L_i	Lengths of the virtual primary and the *ith* secondary backbones measured from the base ring to the end ring.
d_i	Diameter of the *ith* secondary backbone
$\rho(s), \rho_i(s_i)$	Radius of curvature of the primary and the *ith* secondary backbones.
$\theta(s)$	The angle of the tangent to the virtual primary backbone in the bending plane. $\theta(L)$ and $\theta(0)$ are designated by θ_L and θ_0, respectively. $\theta_0 = \pi/2$.
δ_i	A right-handed rotation angle about $\hat{\mathbf{z}}_1$ from $\hat{\mathbf{x}}_1$ to a ray passing through the virtual primary backbone and the *ith* secondary backbone.
δ	$\delta \equiv \delta_1$ and $\delta_i = \delta + \beta_i$.
$\boldsymbol{\psi}$	$\boldsymbol{\psi} \equiv [\theta_L \;\; \delta]^T$ defines the configuration of the brace.

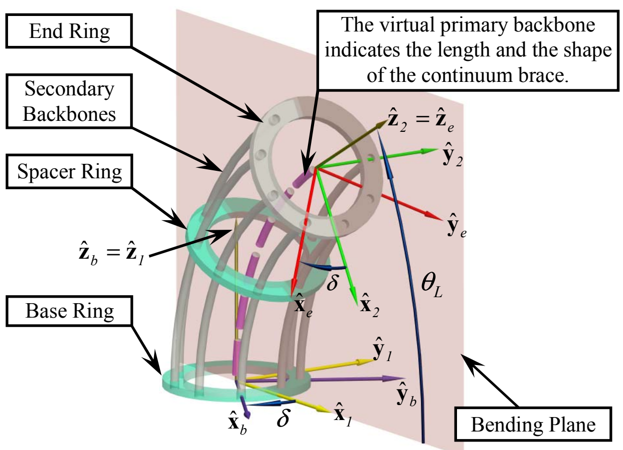

Fig. 2. Nomenclature and coordinates of the continuum shoulder brace

B. Kinematics

Thorough kinematics analysis of such a continuum brace can be found in [29, 31, 32]. This kinematics holds for the following three scenarios: i) the primary-backbone shape is not circular; ii) the primary-backbone length is not constant; and iii) the r_i and β_i values can arbitrarily assigned.

Configuration of the continuum brace is parameterized by $\boldsymbol{\psi} = [\theta_L \;\; \delta]^T$. Since shapes of the secondary backbones are assumed by a sweeping motion of the structure's cross section along the primary backbone, projection of the *ith* secondary backbone on the bending plane is a curve which is offset by Δ_i from the primary backbone. Its radius of curvature and arc-length are indicated by $\rho_i(s_i)$ and s_i. $\rho(s)$ and $\rho_i(s_i)$ are related as follows:

$$\rho(s) = \rho_i(s_i) + \Delta_i \tag{1}$$

Where $\Delta_i \equiv r_i \cos\delta_i$.

L is related to L_i according to:

$$L_i = \int ds_i = \int (ds_i - ds + ds) = L + \int (ds_i - ds) \tag{2}$$

Referring to Fig. 2, the integral above can be rewritten as in Eq. (3). Substituting Eq. (1) into Eq. (3) gives Eq.(4), which leads to the result as in Eq. (5):

$$\int (ds_i - ds) = \int_0^{\theta_0 - \theta_L} \left(\rho_i(s_i) - \rho(s)\right) d\theta \tag{3}$$

$$\int_0^{\theta_0 - \theta_L} \left(\rho_i(s_i) - \rho(s)\right) d\theta = -\int_0^{\theta_0 - \theta_L} \Delta_i d\theta \tag{4}$$

$$L_i = L - r_i \cos\delta_i (\theta_0 - \theta_L) = L + r_i \cos\delta_i (\theta_L - \theta_0) \tag{5}$$

Tip position ${}^b\mathbf{p}_L$ of the continuum brace is given by:

$${}^b\mathbf{p}_L = {}^b\mathbf{R}_1 \left[\int_0^L \cos(\theta(s)) ds \;\; 0 \;\; \int_0^L \sin(\theta(s)) ds \right]^T \tag{6}$$

Where ${}^b\mathbf{R}_1 = \mathrm{R}(\hat{\mathbf{z}}_b, -\delta)$ and the integrals depend on the actual shape of the primary backbone.

The shoulder brace is actuated by pushing and pulling the secondary backbones. According to Eq. (5), L_i depends on L, θ_L and δ. When the continuum exoskeleton is worn on patients with different shoulder widths, the actual shape of the primary backbone would also be different, as indicated by the simplified diagram as in Fig. 3.

If L is constant, the arm sleeve would still slide up and down along the axis of the upper arm for different arm orientations. If the arm sleeve is firmly connected to the upper arm for assistances, L must be actively changed.

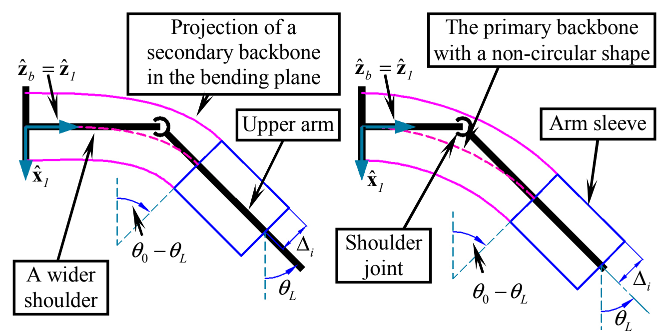

Fig. 3. A schematic diagram for the shoulder exoskeleton while worn on patents with different shoulder widths

IV. System Descriptions

System components of this continuum exoskeleton mainly include the continuum braces, the arm sleeves and the transmission units. Their descriptions are presented.

A. The continuum shoulder brace

As shown in Fig. 4, the secondary backbones are passed through the base ring, the spacer rings and attached to the end ring. Their push-pull actuations bend and/or extend/shorten the continuum shoulder brace.

Main design parameters of the continuum brace include length range of the virtual primary backbone (L), size and placement of the secondary backbones (d_i, r_i and β_i). Determination of these parameters was primarily based on the functionality and usability of this design.

As mentioned in [33], a shoulder joint provides a torque as high as 10 Nm to drive the upper limb during ADLs (Activities of Daily Living). The design of the shoulder brace should firstly be strong enough. Suggested by a simplified statics model in [28] and verified by the experiments in [29], this design continues with a similar arrangement to use 24 secondary backbones at diameters of 1.2mm ($d_i = 1.2mm$).

If the redundant secondary backbones are used, each backbone could be thinner. The use of more and thinner backbones brings a few additional advantages: i) thinner backbones increase the brace's flexibility hence potentially leads to a increased user comfort; ii) failure of one thin backbone would not disable the entire brace hence reliability and safety can also be potentially increased.

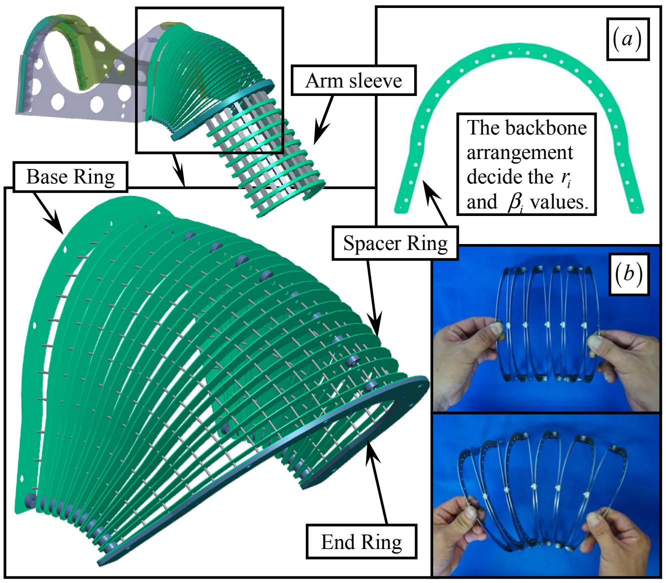

Fig. 4. The continuum shoulder brace: (a) the backbones arrangement, (b) the riveted spacer rings

The r_i and β_i values indicate the backbone arrangement, which is shown in Fig. 4(a). The considerations led to this arrangement include three aspects: i) the backbones shall surround the arm to orient the arm towards an arbitrary direction; ii) the brace could be easily put on a patient; and iii) the brace is big enough to fit a reasonable group of patients.

The spacer rings with holes for the backbones were hence fabricated using stainless steel. As shown in Fig. 4(b), the adjacent rings are riveted to keep them evenly distributed when the brace is bent or extended.

The elasticity of the riveted spacer rings allows the extension or contraction of the continuum brace, as shown in Fig. 4(b). The length of the virtual primary backbone (L) hence can vary between 100 mm and 180 mm.

B. *The arm sleeve*

The arm sleeve is a rigid structure which will be firmly attached to the wear's arm. Then the torque generated from the bending of the brace will assist one's arm motions.

As shown in Fig. 7 and Fig. 8, the inflatable bandages were wrapped around the arms at first. Then the hook-and-loop fasteners were used to attach the bandages to the arm sleeve. The bandages were then inflated to swathe the arm, forming a firm attachment between the arm and the arm sleeve.

A human shoulder allows i) the abduction/adduction motion in the coronal plane, ii) the flexion/extension motion in the sagittal plane, and iii) the medial/lateral rotation of the arm (rotation about the axis of the upper arm). But the continuum brace only undergoes a 2-DoF bending. The arm sleeve was hence designed long enough for the elbows to fully extend. Then the unassisted medial/lateral rotation of the arm will not cause unexpected results.

C. *The transmission unit*

Actuation of the continuum brace involves simultaneous pushing and pulling of the 24 secondary backbones according to the actuation kinematics as in Eq. (5).

If the arm brace is firmly attached to the arm, L will not be kept a constant. The 24 actuation lengths depend on three variables (L , δ and θ_L). If only a unilateral assistance is intended, a complicated actuation unit will be needed. This actuation unit either has 24 motors for the desired push-pull actuation, or has a complex transmission system to generate 24 outputs from 3 inputs.

The bilateral symmetric design of the current exoskeleton from Fig. 1 eliminated such a complex actuation unit, making full use of the backdrivability of the shoulder brace.

No matter what configuration one shoulder brace is at, as long as the motions are symmetric, the push-pull actuation of one backbone in this brace is always equal to the desired actuation length of the corresponding backbone in the other continuum brace.

The transmission was then designed to realize this synchronous motion. As shown in Fig. 5, two backbones, from the right and the left braces respectively, were rigidly connected and they both slide in a slot. If the right brace was active and the right-brace backbone was pushed or pulled, the left-brace backbone would be pushed or pulled for the same length. Motions of the active brace were then transmitted to drive the other brace.

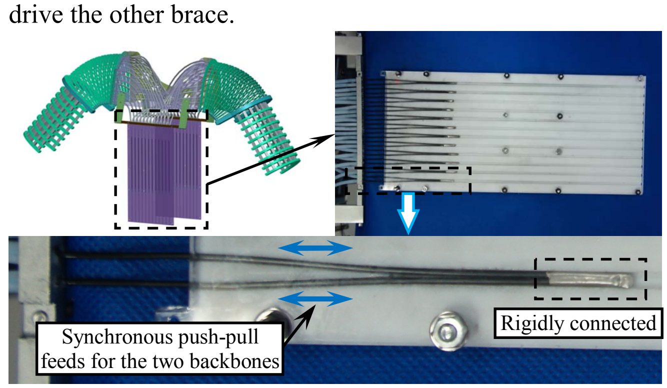

Fig. 5. The transmission unit

V. PRELIMINARY EXPERIMENTAL RESULTS

In order to demonstrate the effectiveness of the proposed continuum shoulder exoskeleton, a series of experiments were conducted on a mockup patient and on a human subject. Although the bilateral movements were all realized to some extent, considerable frictional resistances existed within the system due to too many sliding relative movements with in the design. The resistances lowered the performance.

A. Trials on a mockup patient

The shoulder exoskeleton was put on a mockup patient that is shown in Fig. 6. Three serially connected revolute joints approximate the shoulder joint since a standard spherical joint doesn't have enough motion ranges. Axes of these revolute joints intersect at a point which is the center of the shoulder joint. The shoulder width can be changed between 370mm and 460mm by turning a lead screw.

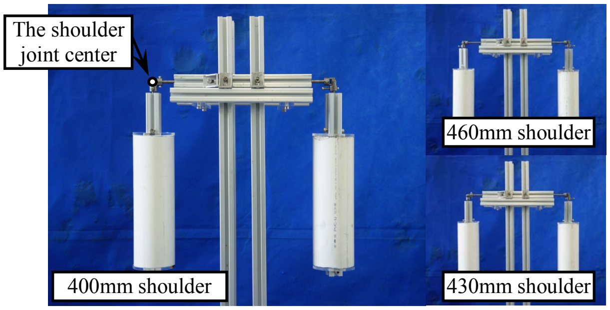

Fig. 6. The mockup patient with a variable shoulder width

The shoulder exoskeleton was put on the mockup patient with a 400mm wide shoulder. As shown in Fig. 7, the mockup arms were attached to the arm sleeve using the inflatable bandages and the hook-and-loop fasteners. One arm was manually posed and the other arm was driven to a similar orientation, as shown in Fig. 7(b) to (d) and in the multimedia extension. Discrepancy in orientations is between 5º to 10º.

Similar results were obtained for the 430mm and 460mm shoulder widths.

B. Trials on a healthy human subject

The continuum shoulder exoskeleton was then put on a healthy human subject to demonstrate the effectiveness of the proposed idea. The current design could be easily worn even for impaired subjects. Bilateral motions can be viewed in Fig. 8 as well as in the multimedia extension. According to the human wearer, he can feel the assistance to one arm delivered via the exoskeleton by the other arm.

VI. Conclusion and Future Work

This paper presents a continuum shoulder exoskeleton design for rehabilitation. Confirmed by previous results in [29] and the new experimental validation, the design's intrinsic flexibility allow its shape adaption to different patient anatomies passively to assist a group of patients without requiring any hardware adjustments. Besides the feature of providing AAA (Anatomy Adaptive Assistances), the design also has a unique symmetric structure to realize self-provided bilateral trainings. Making full use of the backdrivability of the continuum brace, motions of the unaffected healthy side can be transmitted to drive the affected hemiparetic side.

The design and preliminary experimentation are elaborated. The experiments on a mockup patient and a human subject validated the proposed idea.

Immediate future work will focus on improving the performance of the current design, since there are considerable frictional resistances during the two braces' bilateral movements. Based on the encouraging experimental results from this paper and the feasibility study in [34], the long-term future work is to stack more continuum braces to build a safe, light, multiple-DoF exoskeleton for the entire arm. With the new exoskeleton built, clinical effectiveness of bilateral trainings could be further evaluated and new rehabilitation strategies could be developed.

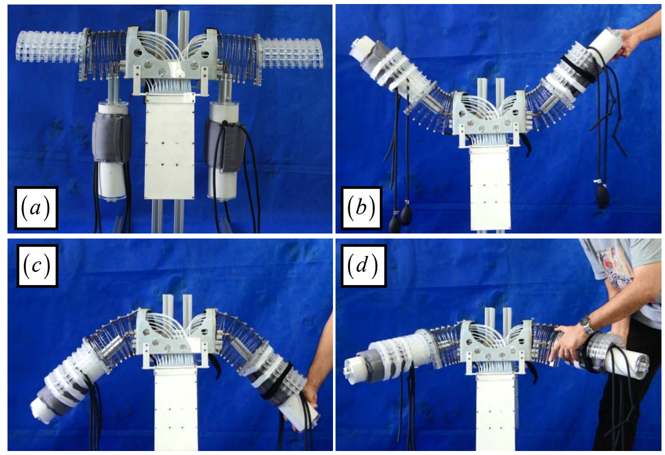

Fig. 7. Bilateral motions of the mockup patient using the exoskeleton: (a) before the arms were attached, (b) to (d) various bilateral movements

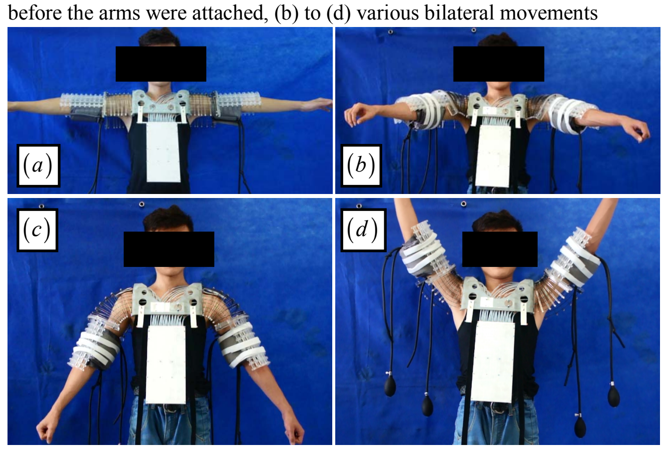

Fig. 8. Bilateral motions of a human subject: (a) before the arms were attached, (b) to (d) various bilateral movements

References

[1] A. M. Dollar and H. Herr, "Lower Extremity Exoskeletons and Active Orthoses: Challenges and State-of-the-Art," *IEEE Transactions on Robotics,* vol. 24, No.1, pp. 144-158, Feb 2008.

[2] A. B. Zoss, H. Kazerooni, and A. Chu, "Biomechanical Design of the Berkeley Extremity Exoskeleton (BLEEX)," *IEEE/ASME Transaction on Mechatronics,* vol. 11, No.2, pp. 128-138, April 2006.

[3] C. J. Walsh, D. Paluska, K. Pasch, W. Grand, A. Valiente, and H. Herr, "Development of a Lightweight, Underactuated Exoskeleton for Load-Carrying Augmentation," in *IEEE International Conference on Robotics and Automation (ICRA)*, Orlando, Florida, USA, 2006.

[4] M. Bergamasco, F. Salsedo, S. Marcheschi, N. Lucchesi, and M. Fontana, "A Novel Compact and Lightweight Actuator for Wearable Robots," in *IEEE International Conference on Robotics and Automation (ICRA)*, Anchorage, Alaska, USA, 2010, pp. 4197-4203.

[5] Y. Sankai, "HAL: Hybrid Assistive Limb Based on Cybernics," in *Robotics Research*. vol. 66, M. Kaneko and Y. Nakamura, Eds.: Springer Berlin Heidelberg, 2011, pp. 25-34.

[6] S. K. Banala, S. K. Agrawal, A. Fattah, V. Krishnamoorthy, W.-L. Hsu, J. Scholz, and K. Rudolph, "Gravity-Balancing Leg Orthosis and Its Performance Evaluation," *IEEE Transactions on Robotics,* vol. 22, No.6, pp. 1228-1239, 2006.
[7] J. F. Veneman, R. Ekkelenkamp, R. Kruidhof, F. C. T. van der Helm, and H. van der Kooij, "A Series Elastic- and Bowden-Cable-Based Actuation System for Use as Torque Actuator in Exoskeleton-Type Robots," *International Journal of Robotics Research,* vol. 25, No.3, pp. 261-281, March 2006.
[8] J. A. Saglia, N. G. Tsagarakis, J. S. Dai, and D. G. Caldwell, "A High Performance 2-dof Over-Actuated Parallel Mechanism for Ankle Rehabilitation," in *IEEE International Conference on Robotics and Automation (ICRA)*, Kobe, Japan, 2009, pp. 2180-2186.
[9] R. J. Farris, H. A. Quintero, and M. Goldfarb, "Preliminary Evaluation of a Powered Lower Limb Orthosis to Aid Walking in Paraplegic Individuals," *IEEE Transactions on Neural Systems and Rehabilitation Engineering,* vol. 19, No.6, pp. 652-659, Dec 2011.
[10] N. G. Tsagarakis and D. G. Caldwell, "Development and Control of a 'Soft-Actuated' Exoskeleton for Use in Physiotherapy and Training," *Autonomous Robots,* vol. 15, No.1, pp. 21-33, 2003.
[11] J. C. Perry, J. Rosen, and S. Burns, "Upper-Limb Powered Exoskeleton Design," *IEEE/ASME Transaction on Mechatronics,* vol. 12, No.4, pp. 408-417, Aug 2007.
[12] A. Gupta, M. K. O'Malley, V. Patoglu, and C. Burgar, "Design, Control and Performance of RiceWrist: A Force Feedback Wrist Exoskeleton for Rehabilitation and Training," *International Journal of Robotics Research,* vol. 27, No.2, pp. 233-251, Feb 2008.
[13] A. H. A. Stienen, E. E. G. Hekman, G. B. Prange, M. J. A. Jannink, A. M. M. Aalsma, F. C. T. v. d. Helm, and H. v. d. Kooij, "Dampace: Design of an Exoskeleton for Force-Coordination Training in Upper-Extremity Rehabilitation," *Journal of Medical Devices,* vol. 3, No.031003, pp. 1-10, Sept 2009.
[14] J. Klein, S. Spencer, J. Allington, J. E. Bobrow, and D. J. Reinkensmeyer, "Optimization of a Parallel Shoulder Mechanism to Achieve a High-Force, Low-Mass, Robotic-Arm Exoskeleton," *IEEE Transactions on Robotics,* vol. 26, No.4, pp. 710-715, Aug 2010.
[15] E. T. Wolbrecht, D. J. Reinkensmeyer, and J. E. Bobrow, "Pneumatic Control of Robots for Rehabilitation," *International Journal of Robotics Research,* vol. 29, No.1, pp. 23-38, Jan 2010.
[16] S. K. Agrawal, V. N. Dubey, J. J. Gangloff, E. Brackbill, Y. Mao, and V. Sangwan, "Design and Optimization of a Cable Driven Upper Arm Exoskeleton," *Journal of Medical Devices,* vol. 3, No.031004, pp. 1-8, Sept 2009.
[17] Y. Mao and S. K. Agrawal, "Design of a Cable-Driven Arm Exoskeleton (CAREX) for Neural Rehabilitation," *IEEE Transactions on Robotics,* vol. 28, No.4, pp. 922-931, Aug 2012.
[18] H. I. Krebs, N. Hogan, M. L. Aisen, and B. T. Volpe, "Robot-Aided Neurorehabilitation," *IEEE Transactions on Rehabilitation Engineering,* vol. 6, No.1, pp. 75-87, March 1998.
[19] C. G. Burgar, P. S. Lum, P. C. Shor, and H. F. M. V. d. Loos, "Development of Robots for Rehabilitation Therapy: the Palo Alto VA/Stanford Experience," *Journal of Rehabilitation Research and Development,* vol. 37, No.6, pp. 663-673, Dec 2000.
[20] P. S. Lum, C. G. Burgar, M. van der Loos, P. C. Shor, M. Majmundar, and R. Yap, "MIME Robotic Device for Upper-Limb Neurorehabilitation in Subacute Stroke Subjects: A Follow-up Study " *Journal of Rehabilitation Research & Development,* vol. 43, No.5, pp. 631-642, Aug 2006.
[21] B. R. Brewer, S. K. McDowell, and L. C. Worthen-Chaudhari, "Poststroke Upper Extremity Rehabilitation: A Review of Robotic Systems and Clinical Results," *Topics in Stroke Rehabilitation,* vol. 14, No.6, pp. 22-44, Nov 2007.
[22] S. Hesse, H. Schmidt, and C. Werner, "Machines to Support Motor Rehabilitation after Stroke: 10 Years of Experience in Berlin," *Journal of Rehabilitation Research and Development,* vol. 43, No.5, pp. 671-678, 2006.
[23] A. R. Luft, S. McCombe-Waller, J. Whitall, L. W. Forrester, R. Macko, J. D. Sorkin, J. B. Schulz, A. P. Goldberg, and D. F. Hanley, "Repetitive Bilateral Arm Training and Motor Cortex Activation in Chronic StrokeA Randomized Controlled Trial," *The Journal of the American Medical Association,* vol. 292, No.15, pp. 1853-1861, Oct 2004.
[24] S. J. Page, V. Hill, and S. White, "Portable Upper Extremity Robotics is as Efficacious as Upper Extremity Rehabilitative Therapy: a Randomized Controlled Pilot Trial," *Clinical Rehabilitation,* vol. 27, No.6, pp. 494-503, June 2013.
[25] H. Kim, L. M. Miller, N. Byl, G. M. Abrams, and J. Rosen, "Redundancy Resolution of the Human Arm and an Upper Limb Exoskeleton," *IEEE Transactions on Biomedical Engineering,* vol. 59, No.6, pp. 1770-1779, June 2012.
[26] N. Jarrassé and G. Morel, "Connecting a Human Limb to an Exoskeleton," *IEEE Transactions on Robotics,* vol. 28, No.3, pp. 697-709, June 2012.
[27] H. Kobayashi and K. Hiramatsu, "Development of Muscle Suit for Upper Limb," in *IEEE International Conference on Robotics and Automation (ICRA)*, New Orleans, LA, USA, 2004, pp. 2480-2485.
[28] K. Xu, D. Qiu, and N. Simaan, "A Pilot Investigation of Continuum Robots as a Design Alternative for Upper Extremity Exoskeletons," in *IEEE International Conference on Robotics and Biomimetics (ROBIO)*, Phuket, Thailand, 2011, pp. 656-662.
[29] K. Xu and D. Qiu, "Experimental Design Verification of a Compliant Shoulder Exoskeleton," in *IEEE International Conference on Robotics and Automation (ICRA)*, Karlsruhe, Germany, 2013, p. accepted for presentation.
[30] S. Hesse, G. Schulte-Tigges, M. Konrad, A. Bardeleben, and C. Werner, "Robot-Assisted Arm Trainer for the Passive and Active Practice of Bilateral Forearm and Wrist Movements in Hemiparetic Subjects," *Archives of Physical Medicine and Rehabilitation,* vol. 84, No.6, pp. 915-920, June 2003.
[31] K. Xu and N. Simaan, "Analytic Formulation for the Kinematics, Statics and Shape Restoration of Multibackbone Continuum Robots via Elliptic Integrals," *Journal of Mechanisms and Robotics,* vol. 2, Feb 2010.
[32] R. J. Webster and B. A. Jones, "Design and Kinematic Modeling of Constant Curvature Continuum Robots: A Review " *International Journal of Robotics Research,* vol. 29, No.13, pp. 1661-1683, Nov 2010.
[33] J. Rosen, J. C. Perry, N. Manning, S. Burns, and B. Hannaford, "The Human Arm Kinematics and Dynamics during Daily Activities - toward a 7 DOF Upper Limb Powered Exoskeleton," in *IEEE International Conference on Advanced Robotics (ICAR)*, Seattle, WA, 2005, pp. 532-539.
[34] K. Xu, Y. Wang, and D. Qiu, "Design Simulations of the SJTU Continuum Arm Exoskeleton (SCAX)," in *International Conference on Intelligent Robotics and Applications (ICIRA)*, Busan, Korea, 2013, p. Submitted.